Published in final edited form as:
J Dent Res. 2005 April ; 84(4): 365–370.

Discontinuous Fiber-reinforced Composites above Critical Length

R.C. Petersen
University of Alabama at Birmingham, School of Engineering, Department of Biomedical Engineering, Hoehn Building, Room 330, 1075 South 13th Street, Birmingham, AL 35294, USA

R.C. Petersen: rpetersen@cs1.dental.uab.edu

Abstract

Micromechanical physics of critical fiber length, describing a minimum filament distance for resin impregnation and stress transfer, has not yet been applied in dental science. As a test of the hypothesis that 9-micron-diameter, 3-mm-long quartz fibers would increase mechanical strength over particulate-filled composites, photocure-resin-pre-impregnated discontinuous reinforcement was incorporated at 35 wt% into 3M Corporation Z100, Kerr Corporation HerculiteXRV, and an experimental photocure paste with increased radiopaque particulate. Fully articulated four-point bend testing *per* ASTM C 1161-94 for advanced ceramics and Izod impact testing according to a modified unnotched ASTM D 256-00 specification were then performed. All photocure-fiber-reinforced composites demonstrated significant improvements over particulate-filled compounds ($p < 0.001$) for flexural strength, modulus, work of fracture, strain at maximum load, and Izod toughness, with one exception for the moduli of Z100 and the experimental reinforced paste. The results indicate that inclusion of pre-impregnated fibers above the critical aspect ratio yields major advancements regarding the mechanical properties tested.

Keywords

critical length; critical aspect ratio; discontinuous

INTRODUCTION

Since initial commercialization, dental composites have improved, particularly in terms of wear, primarily through reductions in the size of the particulate filler (American Dental Association [ADA] Council on Scientific Affairs, 1998). Nevertheless, strengths are inadequate to an extent that composites cannot be recommended for use in stress-bearing contact areas (ADA Council on Scientific Affairs, 1998). Although few references are found regarding dental glass microfibers, a current state-of-the-art commercial photocure composite uses low amounts of fiber filler at 40- to 60-micron lengths and 6- to 10-micron diameters for minor aspect ratios (lengths/diameters) of just 4–10 (Clinical Research Associates, 1998). However, it is widely recognized, for fiber-reinforced materials, that strengths for particulate-filled compounds are minimal compared with high-aspect-ratio composites attaining sufficient oriented lengths and properly bonded for stress transfer within the polymer matrix (Bascom, 1987; Mallick, 1997; Chawla, 1998; Wypych, 1999). Such discontinuous fibers, from 0.5 mm in length upward, when placed into resin

subsequently supplied as bulk, pellet, or sheet forms, are commonly applied throughout industry for polymerized molding of complex curved parts (Bascom, 1987). In fact, high-aspect-ratio fibers previously investigated for increasing dental composite consistency allow for conventional amalgam alloy condensation (Petersen, 2001). Heightened packing by 3.0-mm fiber-reinforced composite consequently allows for routine re-establishment of the interproximal contact, in addition to a consolidating reduction of voids (Petersen, 2001), considered to be among the major complaints by practicing dentists for class II composites (Christiansen, 1997).

Critical length (L_c) is a measure of the minimum perfectly aligned fiber dimension required for maximum stress transfer within the cured resin (Cox, 1952; Kelly and Tyson, 1965; Chawla, 1998). By maximizing fiber-aspect ratio, one can reduce the debonding effects of high-modulus filament end-shear through the polymer, so that composite strengths are increased (Cox, 1952; Kelly and Tyson, 1965; Chawla, 1998). The major factors that influence oriented L_c include the interfacial shear bond strength (τ) between the fiber and resin, the fiber tensile strength (σ_f), and the fiber diameter (d) (Kelly and Tyson, 1965; Chawla, 1998). Critical lengths can be approximated for a vinyl ester equivalent to the standard dental resin 2,2-bis [p-(2′hydroxy-3′-methacryloxypropoxyphenyl)] propane (Bis-GMA) with styrene applied as the diluent monomer from fiber fragmentation tests ranging between 0.5 and 1.6 mm, with E-glass filaments (Cheng *et al.*, 1993). The National Institute of Standards and Technology (NIST) investigated τ for a 70:30 ratio Bis-GMA:triethylene glycol dimethacrylate (TEGDMA) photocure dental resin system with 16.0-micron-diameter E-glass filaments silanated by 3-methacryloxypropyltrimethoxysilane (MPTMS) (McDonough *et al.*, 2001). E-glass is a customary high-tensile-strength silica-based fiber having a common pristine σ_f at 3.4 GPa (Gauthier, 1995), which can be used as an estimate with the NIST investigation, where all tests producing fiber breakage were discarded. The average perfectly aligned NIST value for τ was calculated to be 33.8 MPa, so, with the following basic formula from critical length interfacial theory (Kelly and Tyson, 1965; Chawla, 1998):

$$\tau = \sigma_f d/2L_c \text{ or } L_c = \sigma_f d/2\tau$$

A 16.0-micron-diameter E-glass L_c can be estimated to be approximately 800 microns in a photocure Bis-GMA dental resin system, for a L_c/d critical aspect ratio of 50. Therefore, unaligned dental microfiber lengths with minimal aspect ratios and resulting isotropic orientations have been unable to provide any substantial reinforced strength increases for a vinyl ester Bis-GMA:TEGDMA composite.

Once fibers attain a critical length for a specific composite resin system, most other properties are similarly improved with increasing aspect ratio. As fibers lengthen relative to their diameters, strengths (tensile, flexural, fatigue), modulus, and toughness (impact, fracture toughness) all increase (Bascom, 1987; Mallick, 1997; Chawla, 1998; Wypych, 1999). Reduced overall polymerization shrinkage occurs with increasing aspect ratio, particularly along the fiber axis (Cloud and Wolverton, 1978; Wypych, 1999), with less shrinkage stress and lower creep (Wypych, 1999). Wear improves in conjunction with

underlying mechanical strength properties that support loading, particularly as the reinforcement length extends beyond the average plowing groove (Giltrow, 1973; Friedrich, 1993). Fibers can also be used as a carrier mechanism for structural adhesives to control bondline thickness/pressure and raise toughness (Bolger, 1983; Shetty and Spearing, 1997).

As a demonstration of the hypothesis that 3.0-mm discontinuous fiber reinforcement will improve mechanical strengths over those of particulate-filled dental composites, photocure-resin-pre-impregnated high-purity quartz fibers were added at 35 wt% to 2 universal dental composites, 3M Corp. Z100 and Kerr Corp. Herculite XRV. Since quartz is radiolucent and reduces x-ray density as it is added to a material, an experimental paste with 66.8 wt% barium silicate glass was investigated for incorporation of 35 wt% discontinuous quartz fiber. Fully articulated four-point bend and unnotched Izod impact were chosen as mechanical tests to prove the hypothesis. The marginal level of uncertainty was set at $p < 0.001$.

MATERIALS & METHODS

Materials

High-purity 99.99% silica quartz fibers, with uniform 3.0-millimeter lengths by 9.0-micron diameters, coupled with a dimethacrylate-compatible silane (Quartz Products Company, Lexington, KY, USA), were impregnated with Bis-GMA resin and TEGDMA monomer (Esschem, Essington, PA, USA). Photochemicals and additives were formulated as follows for the final resin systems: photo-oxidants camphorquinone (Aldrich, Milwaukee, WI, USA), 0.4 wt%, and Irgacure 819 (Ciba, Tarrytown, NY, USA), 1.0 wt%; and photo-reductant 2-dimethylaminoethyl methacrylate (Aldrich, Milwaukee, WI, USA), 0.8 wt%. An initial 50:50 Bis-GMA:TEGDMA resin concentration was used to introduce photochemicals and additives. TEGDMA levels were then reduced to 2.2 wt% by Bis-GMA addition, thereby preventing resin-rich areas from developing away from the fibers during consolidation. Diminished TEGDMA levels are thought to reduce the potential for bacterial colonization related to low-molecular-weight monomers (Hansel *et al.*, 1998). Development proceeded with an ultra-high-viscosity resin heated at 80°C for impregnation of 70 wt% quartz fibers by being mixed with 1.5 wt% anhydrous MgO (Magox, Middleburg Heights, OH, USA) and 4.0 wt% 510 fumed silica (Cabot, Tuscola, IL, USA) for increased thickening. Samples were then pressed and rolled.

An experimental paste consisting of Bis-GMA:TEGDMA in a 3:1 ratio, with the previously described photochemicals at the same concentration levels, was filled with barium glass Ba-45 particulate (Industrial Corp., Lionville, PA, USA) at 66.8 wt%, plus 510 fumed silica 8.2 wt%, adjusted to shade A2 with white pigment 1.3 wt% (Sartomer, West Chester, PA, USA). The barium glass, with an average particle size of 1.5 microns, was previously silanated with 1.0 wt% MPTMS (Dow Corning, Midland, MI, USA) in 70% 2-propanol, dried overnight, and heated briefly at 120°C. Photocure-resin-pre-impregnated discontinuous fibers were incorporated at 50 wt% into Z100 A2 (3M Corporation, St. Paul, MN, USA), XRV A2 (Kerr Corporation, Orange, CA, USA), and the experimental A2 paste for final 35 wt% fiber compositions with the use of pressure in a mortar and on a glass slab, followed by rolling. The universal Z100 and XRV commercial controls had filler volume

percentages of 68 and 56, respectively, and both contained Bis-GMA:TEGDMA photocure resin systems with average particle sizes of 0.6 microns (Lee *et al.*, 2000).

Sample Preparation

Specimens were prepared from the resultant 3 fiber-reinforced composite groups according to American National Standards Institute (ANSI)/ADA specification #27, with a 25×2×2-mm split mold. Fiber-reinforced composites are fully condensable and readily consolidate during placement. Samples were irradiated at 400 mW/cm^2, with a peak wavelength of 470 nanometers monitored by a Demetron radiometer at equivalent times according to manufacturers' recommendations. Specimens from the 2 control groups, Z100 and XRV, were prepared meticulously and similarly photocured. After samples were separated from the mold, excess flash was removed, followed by a finishing sequence with 320-, 600-, and 600-grit wet silicon carbide paper. Polymerized specimens were numbered, separated into 5 different test groups, and measured for depth and width to the nearest 0.0001 inches. Samples having any minor visual defects, x-ray voids, or notable parallelism deviations were discarded.

Mechanical Testing

Fully articulated four-point bend fixtures were machined according to ASTM C 1161-94 specifications for A-sized advanced ceramics with a 20-mm span length and ¼-point 10-mm-spaced loading noses (Petersen and Wenski, 2002). An Instron inspection machine with crosshead speed of 0.5 mm/min was used for the mechanical testing of maximum bend strength for 10 specimens from each of the 5 groups. The following formulae were used to calculate:

$$\textit{Flexural strength}\ (\mathrm{S_F}){:}\mathrm{S_F}=3\mathrm{FL}/4\mathrm{bd}^2\ (\mathrm{ASTM\ C\ 1161-94})$$
$$\textit{Flexural modulus}\ (\mathrm{E_F}){:}\mathrm{E_F}=0.17\mathrm{L}^3\mathrm{M}/\mathrm{bd}^3\ (\mathrm{ASTM\ D\ 6272-00})$$
$$\textit{Strain}\ (\mathrm{r}){:}\mathrm{r}=(4.36\,\mathrm{Dd})/(\mathrm{L}^2)\ (\mathrm{ASTM\ D\ 6272-00})$$

with F = load, L = span length, b = sample width, d = sample depth, M = slope of the tangent to the initial straight line on steepest part of the load deflection curve, r = maximum strain in the outer fibers at midspan, and D = beam deflection.

Work of fracture was integrated for toughness with the use of application software from the load-deflection curve at a maximum of 5% deviation past the peak load.

Energy testing for high strain rate toughness full breakage was accomplished according to a modified ASTM specification D 256-00, with a Tinnius Olsen Plastic Tester and 5 unnotched specimens from each of the 5 test groups. Toughness was calculated as energy *per* unit area at the fracture. Test samples did not meet design criteria and can be used only for comparative purposes.

Densitometer Radiopacity

Five samples from each group were alternated alongside a 99.99% pure aluminum 1-mm incremental stepwedge on Kodak Ectaspeed Plus occlusal film and exposed to 70 KeV at 15

mA from a source distance of 470 mm for 0.20 sec with a General Electric x-ray machine. The x-ray degree of film darkening [(D) = $\log_{10}$ Opacity = 1/transmission] was measured by an X-rite transmission densitometer. Construction of a calibration curve from the stepwedge and requiring posterior composites to attain minimal equivalency of 1.5 or 2.0 mm aluminum/mm composite are variations of ADA Seal Acceptance Guidelines and ANSI/ADA Standard #27 for radiopacity, respectively. The dark radiograph edges were adjusted to 1.6-D, so that composite readings could be measured along the 1.0-D linear region for maximum calibration contrast. The average of 4 readings was used for each specimen tested.

Characterization

X-rays were taken after flexural mechanical testing, identical to densitometer measurements, for fractography observation analysis.

Izod samples surrounding the average median strengths were chosen to image exposed fracture surfaces by scanning electron microscopy (SEM XL30, FEI, Hillsboro, OR, USA).

An atomic force microscope (AFM), Nanoscope III, was used for surface imaging in contact mode for non-sanded, non-fractured samples photocured against a glass slide.

Statistics

Individual test results were statistically analyzed by single-factor one-way Analysis of Variance with Newman-Keuls *post hoc*, with significance set at $p < 0.001$.

RESULTS

Fully Articulated Four-point Flexural Bend

Fully articulated four-point flexural bend test results revealed significant improvements over particulate-filled photocure dental composites by the incorporation of 35wt% discontinuous 3.0-mm fiber over particulate-filled photocure dental composites, with improved flexural strength, flexural modulus, work of fracture, and strain at peak load (Figs. 1A–1D). The mechanical properties of all fiber-reinforced composites tested increased in comparison with those of the 2 commercial particulate-filled controls at a statistically significant level, $p < 0.001$, except for the moduli between the Z100 and the experimental fiber-reinforced paste. The experimental radiopaque paste had significantly lower values than commercial fiber-reinforced composites for flexural modulus, flexural strength, and work of fracture ($p < 0.001$).

X-ray imaging depicts the nature of minor delamination failure for fiber-reinforced composites where fracture originates on the lower tensile surface (Figs. 1E, 1F). All fiber-reinforced samples were intact, with initial tensile failure on the flexural side, showing a common tendency toward fine crack propagation extending inward at the midline or opposite the loading nose up to the neutral axis. The x-rays represent 2 of the most easily identifiable crack failures for imaging from all specimens tested, because of some surface delaminating. Toughness values measured through work of fracture for fiber reinforcement can thus be considered with regard to energy adsorption for a lack of true failure that is

counterbalanced by this characteristic type of lateral fracture damage. By comparison, all commercial particulate-filled dental composites were completely cleaved through in unremarkable smooth brittle failure during maximum bend testing, averaging only about 0.4 microns of tensile deformation elongation across a 20.0-mm span beyond peak load.

Izod Impact Resistance Toughness

All samples broke through completely, producing 2 separate pieces with fractured free ends. Each fiber-reinforced composite group improved Izod impact toughness above that of both commercial particulate-filled controls at a statistically significant level, $p < 0.001$ (Fig. 2A). Relative toughness increases for fiber-reinforced over particulate-filled composites were similar at high-strain-rate testing by Izod impact full breakage, when compared with low-strain-rate work-of-fracture four-point flexural testing (Fig. 1C), with partial crack propagation failure seen radiographically (Figs. 1E, 1F). SEM imaging could be accomplished for samples following Izod testing, since a fracture surface was exposed to illustrate differences between particulate filler (Fig. 2B) and fiber reinforcement (Fig. 2C). The imaging at 5000X depicts toughness improvements for fibers that are in contrast to a larger ductile surface area for debonding energy and fiber fracture, compared with a brittle smooth cleavage surface with particulate filler. Fiber pull-out was observed sporadically at lower magnification.

X-ray Radiopacity

The experimental fiber-reinforced composite with elevated barium silicate particulate increased aluminum equivalent measures of x-ray radiopacity substantially above those of both commercial fiber-reinforced composites, $p < 0.001$ (Table). The experimental fiber-reinforced paste had an aluminum equivalent 7.5% below the adjusted ANSI/ADA Specification #27 for radiopaque requirements and 23% above the ADA Seal Acceptance Guidelines. Both the Z100 and Herculite XRV commercial controls attained aluminum equivalents significantly higher than those of all fiber-reinforced groups, $p < 0.001$. The aluminum stepwedge was calibrated at $r = 0.9850$.

AFM Imaging

A fiber-reinforced composite surface flaw conferred a modulus contrast between the pure quartz silica and cured polymer (Fig. 3). The white identifies the harder quartz fibrils extending upward, displaying dark relief of deeper defects bent through a constrained inner 90° angle. The partially broken fiber defines an approximate outer 90° arc with a 15-micron radius for an otherwise smooth surface, producing an overall surface roughness (Ra) of 16 nm. Particulate-filled paste extruded or squeezed under placement pressure to fill all available space, while fiber ductility assisted in the molding process.

DISCUSSION

Discontinuous resin pre-impregnated fiber reinforcement above critical length represents an important progression for dental materials science. Fiber dimensions can now be realistically examined in terms of critical aspect ratio and bonding, so that stress transfer is optimized within the polymer matrix. The small size of dental fillings will later allow fibers to be

supplied at different lengths, corresponding to cavity dimensions in the range of 1.0–10.0 mm, to increase the percent of continuous strength. Fiber-reinforced composites approaching continuous strengths are then practically projected to provide higher mechanical properties than values from this investigation, where 3.0-mm fibers with 9.0-micron diameters were used across a 20.0-mm span (Mallick, 1997; Chawla, 1998; Wypych, 1999). In addition, the ADA currently advocates smaller fillings, due to the adhesive bonding nature of composites that also requires less tooth undermining (ADA Council on Scientific Affairs, 1998). Thinner cavity widths in addition to longer fibers will thus promote the alignment of fiber planes (Petersen and Wenski, 2002) for higher strength and modulus (Bascom, 1987; Mallick, 1997; Chawla, 1998), which in turn will lead to improvements in other composite properties (Friedrich, 1993; Wypych, 1999).

The use of pure quartz as a fiber is based on quality control development related to critical materials listed under Title III of the Defense Production Act (Strong and Gilbride, 1991). Quartz is considered insoluble, but is extremely hard and difficult to grind, to such an extent that larger jagged particles have previously been identified with a higher rate of wear against enamel (Anusavice, 1996). By comparison, quartz fiber above critical length will align parallel to the occlusal table during compaction placement and should wear by thinning, to peel off as thin sheets through infrequent loss from the resin matrix (Friedrich, 1993); this must be tested for opposing enamel wear.

Surface roughness that encourages inactive micro-areas to support bacterial plaque (Friedrich, 1993; Quirynen and Bollen, 1995) develops in composites over time in the form of wear, marginal chipping, and interfacial porosity (Fukushima *et al.*, 1988; Mazer *et al.*, 1992; Friedrich, 1993). Subsequently, wear is associated with lower modulus, reduced interfacial shear bond strength, and low composite strength, in addition to fibers (with lengths less than the plowing groove) that are easily detached (Friedrich, 1993). Marginal chipping is similarly associated mechanically with lower composite strengths, modulus, and fracture toughness, where internal cure stresses form microcracks which can coalesce after loading (Mazer *et al.*, 1992; Braem *et al.*, 1994; Ferracane and Condon, 1999). In comparison, from the tests during this investigation, fiber reinforcement improved on particle filler by providing exceptionally higher strengths, even greater levels of toughness with energy adsorption, and increased moduli for predicted lower in-service Ra levels. The initial cured composite surface roughness before wear is associated with polishing or the surface against which the material is cured (Friedrich, 1993; Petersen, 2001), where Ra values for both fiber reinforcement or particulate filler are an order of magnitude lower than corresponding techniques used for amalgams (Petersen, 2001). Clinically associated voids are also reduced in reinforced composites when compared with particulate-filled pastes, through a compression process (Petersen, 2001).

Additional clinical advancements can be considered from this study. Extended strength, toughness, and modulus combined should improve dimensional stability along margins to transfer pressure more evenly toward counteracting stress foci from the tooth interface. Reinforced modulus values, approximating those of dentin, 20.7 MPa (Marshall *et al.*, 2001), lower the possibility of detrimental shear stresses due to mismatches in compression along the proximal box. Improved strain properties may prove beneficial when a lateral wall

is lost, as composite filling material goes into tension under Poisson's compressive occlusal force, particularly when interproximal contact is lost. Izod toughness high-strain-rate resistance to critical hyperloading by hard food or foreign material should further protect susceptible margins from chipping. Fiber reinforcement also adsorbs damaging energy or breakage and internal crack propagation, to reduce the possibility of minor or catastrophic failure of over-stressed composites. Strength and modulus are even related to improved wear properties, especially when fibers extend longer than the plowing groove (Giltrow, 1973; Friedrich, 1993).

The experimental fiber-reinforced paste developed to counteract the addition of radiolucent quartz, by incorporating barium silicate glass radiopacity at 33.4 wt%, provided aluminum equivalent levels 92.5% within the ANSI/ADA #27 adjusted materials standard and 23% above the ADA Seal of Acceptance Program Guidelines. TEGDMA diluent concentrations are normally described in a 25–50% range of the polymer mass, with Bis-GMA resin to reduce viscosity (Anusavice, 1996), while the monomer was reduced to approximately 13.6 wt% for the experimental fiber-reinforced paste. Higher TEGDMA levels plus paste vacuum-mixing should improve fiber wetting, crucial in preventing strength-reducing stress-concentrating voids from forming, and allowing higher amounts of radiopaque barium silicate to be added. Ultimately, since TEGDMA promotes bacterial growth (Hansel *et al.*, 1998), monomer limitations are still considered appropriate in future development.

Acknowledgments

Funding sources from the United States Department of Energy Technical Assistance Program and the University of Alabama at Birmingham-sponsored National Institute of Dental and Craniofacial Research Training Grant T32DE14300-02 are respectfully acknowledged. I further express my gratitude to: Jack E. Lemons, University of Alabama at Birmingham, Departments of Orthopedic Surgery, Biomedical Engineering and Prosthodontics and Biomaterials, for composite development; Krishen K. Chawla, University of Alabama at Birmingham, School of Engineering, Department of Materials Science, for micromechanical consultation; Michael S. Reddy, University of Alabama at Birmingham, Department of Periodontics, for periodontal consultation for fiber-reinforced composites; Edward G. Wenski, United States Department of Energy, Kansas City Plant, for mechanical testing; Patrick K. Hardman, X-ray Department, University of Missouri-Kansas City Dental School, for x-rays and densitometer measurement consultation; Vladimir M. Dusevich, Electron Microscope Laboratory, University of Missouri-Kansas City Dental School, for scanning electron microscopy; and Yip-Wah Chung, Director of Materials Science, School of Engineering, Northwestern University, for atomic force microscopy analysis.

References

American Dental Association Council on Scientific Affairs. Statement on posterior resin-based composites. J Am Dent Assoc. 1998; 129:1627–1628. [PubMed: 9818585]

Anusavice, KJ., editor. Phillips' science of dental materials. 10. Philadelphia: W.B. Saunders Company; 1996. Restorative resins. Composite restorative materials; p. 274-282.

Bascom, WD. Other discontinuous fibers. In: Dostal, CA.; Woods, MS.; Frissel, HJ.; Ronke, AW., editors. Composites Engineered materials handbook. Metals Park, OH: ASM International; 1987. p. 119-121.

Bolger, JC. Structural adhesives: today's state of the art. Tape and film adhesives. In: Schneberger, GL., editor. Adhesives in manufacturing. New York: Marcel Dekker, Inc; 1983. p. 148-150.

Braem M, Lambrechts P, Vanherle G. Clinical relevance of laboratory fatigue studies. J Dent. 1994; 22:97–102. [PubMed: 8195483]

Chawla, KK. Composite materials. 2. New York: Springer; 1998. Micromechanics of composites, monotonic strength and fracture, and fatigue and creep; p. 303-346.p. 377-410.

Cheng TH, Jones FR, Wang D. Effect of fibre conditioning on the interfacial shear strength of glass-fiber composites. Compos Sci Technol. 1993; 48(1–4):89–96.

Christiansen GJ. Overcoming challenges with resin in class II situations. J Am Dent Assoc. 1997; 128:1579–1580. [PubMed: 9368445]

Clinical Research Associates. Condensable restorative resins. Clin Res Associates. 1998; 22(7):1.

Cloud PJ, Wolverton MA. Predict shrinkage & warpage of reinforced and filled thermoplastics. Plastic Technol. 1978; 24(11):107–113.

Cox HL. The elasticity and strength of paper and other fibrous materials. Br J Appl Phys. 1952; 3:72–79.

Ferracane JL, Condon JR. In vitro evaluation of the marginal degradation of dental composites under simulated occlusal loading. Dent Mater. 1999; 15:262–267. [PubMed: 10551094]

Friedrich, K., editor. Advances in composite technology. Amsterdam: Elsevier; 1993. Wear models for multiphase materials and synergistic effects in polymeric hybrid composites; p. 209-269.

Fukushima M, Setcos JC, Phillips RW. Marginal fracture of posterior composite resins. J Am Dent Assoc. 1988; 117:577–583. [PubMed: 3066806]

Gauthier, MM., editor. Engineered materials handbook. Metals Park, OH: ASM International; 1995. Fibers, fabrics and reinforcements; p. 505-507.Desk ed

Giltrow JP. Friction and wear of self-lubricating composite materials. Composites. 1973 Mar.:55–64.

Hansel C, Leyhausen G, Mai UE, Geurtsen W. Effects of various resin composite (co)monomers and extracts on two caries-associated micro-organisms *in vitro*. J Dent Res. 1998; 77:60–67. [PubMed: 9437400]

Kelly A, Tyson WR. Tensile properties of fibre-reinforced metals: copper/tungsten and copper/molybdenum. J Mech Phys Solids. 1965; 13:329–350.

Lee SY, Lin CT, Dong DR, Huang HM, Shih YH. Acoustic emissions generated in aged dental composites using a laser themoacoustic technique. J Oral Rehabil. 2000; 27:774–785. [PubMed: 11012853]

Mallick, PK. Random fiber composites. In: Mallick, PK., editor. Composites engineering handbook. New York: Marcel Dekker, Inc; 1997. p. 891-938.

Marshall GW, Habelitz S, Gallagher R, Balooch M, Balooch G, Marshall SJ. Nanomechanical properties of hydrated carious human dentin. J Dent Res. 2001; 80:1768–1771. [PubMed: 11669491]

Mazer RB, Leinfelder KF, Russell CM. Degradation of microfilled posterior composite. Dent Mater. 1992; 8:185–189. [PubMed: 1521708]

McDonough WG, Antonucci JM, Dunkers JP. Interfacial shear strengths of dental resin-glass fibers by the microbond test. Dent Mater. 2001; 17:492–498. [PubMed: 11567686]

Petersen, RC. Chopped fiber reinforced dental material. US Patent. 6, 270,348. 2001 Aug 7.

Petersen, RC.; Wenski, EG. Mechanical testing of a photocured chopped fiber reinforced dental composite. In: Rasmussen, BM.; Pilato, L.; Kliger, HS., editors. Affordable materials technology —platform to global value and performance; 47th International SAMPE Symposium and Exhibition; May 12–16, 2002; Long Beach, CA. Covina, CA: Society for the Advancement of Materials and Process Engineering; 2002. p. 380-394.

Quirynen M, Bollen CM. The influence of surface roughness and surface-free energy on supra and subgingival plaque formation in man. A review of the literature. J Clin Periodontol. 1995; 22:1–14. [PubMed: 7706534]

Shetty SP, Spearing SM. Fracture resistance of a fiber-reinforced film adhesive. Scripta Mater. 1997; 37:787–792.

Strong, KL.; Gilbride, J. Enhancing the US defense industrial base through title III of the Defense Production Act. In: Carri, R.; Poveromo, LM.; Gauland, J., editors. Advanced materials/affordable processes; 23rd International SAMPE Technical Conference; October 21–24, 1991; Kiamecha Lake, NY. Covina, CA: Society for the Advancement of Materials and Process Engineering; 1991. p. 388-402.

Wypych, G., editor. Handbook of fillers. 2. Toronto: Chem Tech Publishing; 1999. Effects of fillers on the mechanical properties of filled materials; p. 395-457.

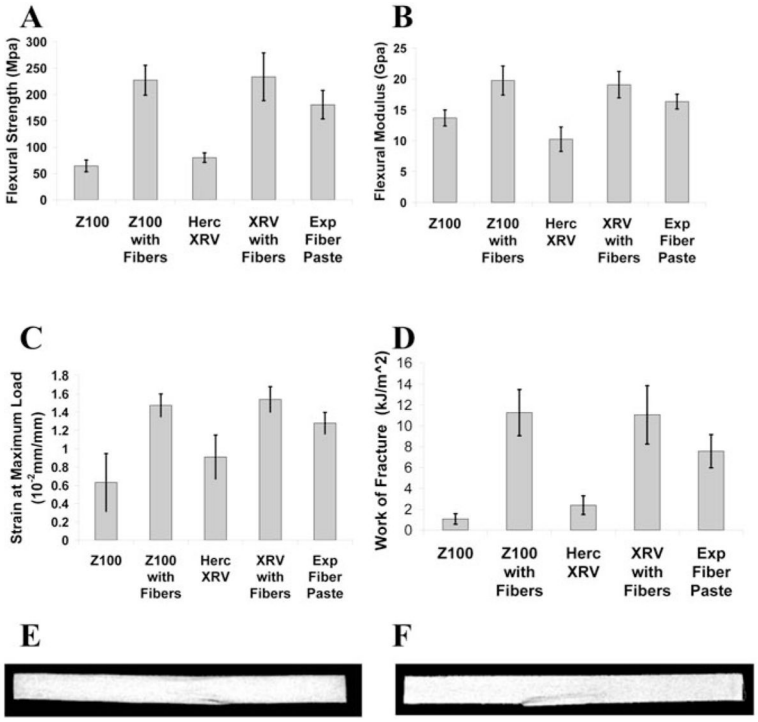

Figure 1.

Fully articulated four-point flexural bend mechanical test results for **(A)** flexural strength, **(B)** flexural modulus, **(C)** strain at peak load, and **(D)** work-of-fracture toughness (each value is the group mean for 10 sample tests; error bars ± 1 standard deviation). X-rays **(E, F)** with two of the most accentuated cracks propagated from all fiber-reinforced samples highlight the common fracture pattern, with initial tensile failure extending back toward the midline and neutral axis. Fiber-reinforced samples were all still intact and supporting a force averaging 60% of the maximum when testing was interrupted, whereas all particulate-filled composites failed immediately at only 0.00002 strain past peak load.

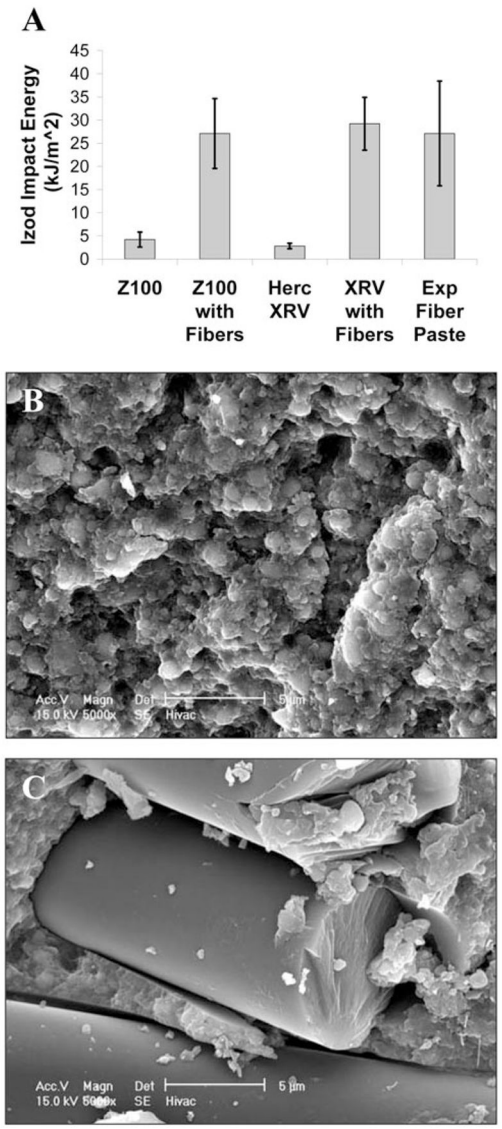

Figure 2.

Izod impact toughness. **(A)** Results for full fracture at high strain rate are charted, demonstrating remarkable toughness improvements when fiber reinforcement is added to particulate-filled dental pastes (each value is the group mean for 5 sample tests; error bars ± 1 standard deviation). **(B)** SEM (scale 5 microns) characterizes particulate-filled commercial composite Z100 with minimal debonding. **(C)** SEM (scale 5 microns) depicts reinforced Z100 with transverse fractured quartz fibers providing a large irregular debonding surface area. Particulate-filled composite essential for fiber-reinforced molding and radiopacity still resides between individual fibrils and as shattered debris.

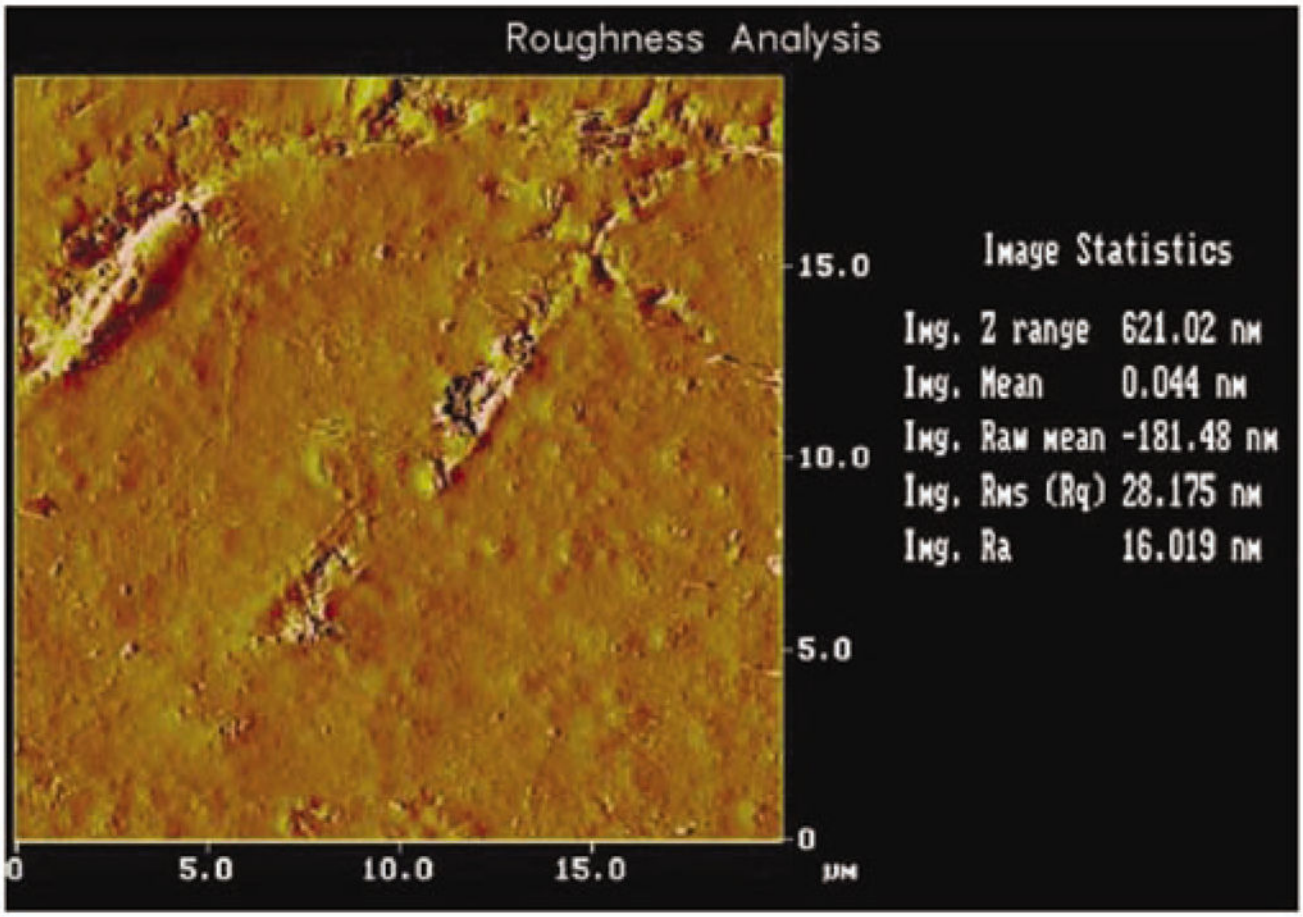

Figure 3.

Atomic force microscope imaging demonstrating the molding ability of a nine-micron-diameter quartz filament by optical laser two-dimensional representation with true statistical information acquired through the three-dimensional counterpart (x-y scales in microns). Rare surface imaging exposes a quartz filament damaged during mixing, placement, and mold separation. Fibrils extending upward provide most of the relief, appearing as white higher-modulus material outlined sporadically by black surrounding deeper defects compared with the large mass of dark greyish particulate-filled paste. Although damage creates an overall vertical Z-range distance of 621 nanometers, due to the ability of the pure quartz fiber to deform by compressing parallel against a surface and particulate paste to fill in space, the average surface roughness is still distinctively only 16 nanometers.

Table

Radiography Densitometer Results

Composite Group	Aluminum Equivalents[a,b,c]
Commercial control, 3M Corp. Z100	2.51 (± 0.09)
3M Z100 + 35 wt% chopped fibers	1.37 (± 0.21)
Commercial control, Kerr Corp. XRV	2.29 (± 0.05)
Kerr Herculite XRV+35 wt% chopped fibers	1.40 (± 0.06)
Exp. paste + 35 wt% chopped fibers	1.85 (± 0.06)

[a] Aluminum equivalents expressed as millimeters of 99.99% pure aluminum thickness *per* millimeter of composite thickness.

[b] ADA Seal of Acceptance Guidelines and ADA Composite Standard #27 for Aluminum Equivalents are 1.5 and 2.0, respectively.

[c] Values are means ± 1 standard deviation of 5 specimens (N = 5).